

## SULFATED FUCOIDAN HYDROGEL FROM *Undaria pinnatifida* AS A HIGH-PERFORMANCE BIOADSORBENT FOR CADMIUM REMOVAL FROM WASTEWATER

Muhammad Azeem<sup>1</sup>, Aqsa Masood<sup>2</sup>, Muhammad Ashraf Shaheen<sup>1\*</sup>, Muhammad Azhar Abbas<sup>2,3</sup>

<sup>1</sup>Faculty of Sciences, Superior University Lahore, Lahore 54000, Pakistan

<sup>2</sup>Institute of Chemistry, University of Sargodha, Sargodha 40100, Pakistan

<sup>3</sup>Government Ambala Muslim Graduate College, Sargodha 40100, Pakistan

### ARTICLE INFO:

#### Keywords:

Sulfated fucoidan hydrogel (FUC-HG), Cadmium removal, Heavy metal adsorption, Freundlich isotherm, Pseudo-second-order kinetics, Chemisorption, Wastewater treatment, Biopolymer adsorbent, Thermodynamics.

#### Corresponding Author:

**Prof. Dr. Muhammad Ashraf Shaheen**

Faculty of Sciences, Superior University Lahore, Lahore 54000, Pakistan:

Email:

[masaheen1964@gmail.com](mailto:masaheen1964@gmail.com)

#### Article History:

Published on December 18, 2025

### ABSTRACT

Cadmium ( $\text{Cd}^{2+}$ ) must be effectively removed from effluent because of its high toxicity and persistence in aquatic settings. In this work, *Undaria pinnatifida* was used to create a sulfated fucoidan hydrogel (FUC-HG), which was then tested as a high-performance bioadsorbent for  $\text{Cd}^{2+}$  sequestration. A maximal adsorption capacity of approximately  $50 \text{ mg g}^{-1}$  was made possible by the hydrogel's heterogeneous surface with numerous active binding sites. While kinetic analysis followed the pseudo-second-order model ( $R^2=0.9876$ ), confirming chemisorption as the main mechanism, equilibrium data fitted the Freundlich isotherm ( $R^2=0.9441$ ), showing multilayer adsorption. According to thermodynamic investigations, the reaction was spontaneous, endothermic, and entropy-driven, which is in line with chemical interactions between the hydroxyl and sulfated functional groups of FUC-HG and  $\text{Cd}^{2+}$  ions. Elovich and intraparticle diffusion investigations, which emphasised surface binding followed by pore diffusion, provided additional evidence for sequential uptake. Over several cycles, the hydrogel showed outstanding durability and reusability while retaining a high adsorption efficiency. These findings establish FUC-HG as an economical, selective, and eco-friendly bioadsorbent with great promise for real-world use in industrial heavy metal remediation and wastewater treatment.

## 1. Introduction

One of the most serious environmental problems brought on by fast industrialisation, mining, electroplating, battery manufacturing, and fertiliser production is heavy metal poisoning of aquatic systems [1]. Cadmium ( $\text{Cd}^{2+}$ ) is one of the most dangerous metals because of its high water mobility, lengthy biological half-life, and extreme toxicity even at low levels [2]. International regulatory bodies have imposed stringent discharge limitations on cadmium due to its association with kidney dysfunction, skeletal damage, carcinogenicity, and ecological bioaccumulation [3]. Nonetheless, a major scientific and technological challenge remains in effectively removing  $\text{Cd}^{2+}$  from complicated effluent streams under practical conditions.

Chemical precipitation, ion exchange resins, membrane filtering, and electrochemical treatments are examples of conventional cadmium removal methods that frequently have disadvantages such as high operating costs, secondary sludge production, limited selectivity, and poor regeneration efficiency [4]. Because of their ease of use, scalability, and ability to adjust to low metal concentrations, adsorption-based methods have become one of the most promising substitutes. However, a lot of reported adsorbents rely on inorganic materials, synthetic polymers, or activated carbons that are not sustainable, need energy-intensive manufacturing processes, or function poorly in changeable wastewater conditions. Growing interest in bio-based, renewable, and ecologically safe adsorbents that can achieve high adsorption efficiency without sacrificing ecological safety has resulted from this [5-16].

Because of their abundance, rich surface chemistry, and intrinsic biodegradability, marine polysaccharides have garnered significant interest as next-generation adsorption materials [17-26]. Fucoidan, a sulfated polysaccharide derived from brown seaweeds like *Undaria pinnatifida*, is especially appealing due to its high density of

hydroxyl ( $-\text{OH}$ ) and sulphate ( $-\text{SO}_3^-$ ) functional group. Fucoidan is a viable option for selective heavy metal binding because of these properties, which offer strong electrostatic interactions and coordination sites for divalent metal ions [27]. However, natural fucoidan's water solubility, poor mechanical stability, and challenges with recovery following adsorption limit its practical usage in wastewater treatment systems.

Fucoidan's structural alteration into a crosslinked hydrogel (FUC-HG) provides a logical way to improve its physicochemical stability while maintaining its inherent metal-binding capability in order to get over these restrictions [28]. Rapid mass transfer, fast water uptake, and active site accessibility are all made possible by hydrogels' three-dimensional porous network. These hydrogels are excellent for aqueous metal remediation because they combine ion-exchange capacity, chemical affinity, and structural robustness when produced from sulfated biopolymers. Despite these benefits, there are still few systematic studies in the literature on sulfated fucoidan-based hydrogels for cadmium adsorption, especially with thorough kinetic, isothermal, thermodynamic, and mechanistic evaluations.

This study generated and assessed a sulfated fucoidan hydrogel (FUC-HG) obtained from *Undaria pinnatifida* as a high-performance bioadsorbent for the removal of  $\text{Cd}^{2+}$  from aqueous environments. The effects of temperature, initial  $\text{Cd}^{2+}$  content, and dosage were investigated by batch adsorption studies [29]. In order to clarify the governing adsorption pathways, the adsorption behaviour was thoroughly examined using a variety of kinetic and isotherm models in addition to thermodynamic and mechanistic interpretations. This work intends to improve the use of marine biopolymer-based hydrogels in cutting-edge wastewater treatment technologies and establish FUC-HG as a practical, environmentally friendly substitute for traditional adsorbents by

combining sustainability, high adsorption efficiency, and reusability.

## 2. Materials and Methods

### 2.1. Materials

The main source of fucoidan was commercially accessible dried brown seaweed (*Undaria pinnatifida*). Sigma-Aldrich provided analytical-grade cadmium nitrate tetrahydrate ( $\text{Cd}(\text{NO}_3)_2 \cdot 4\text{H}_2\text{O}$ ), ethanol ( $\geq 99\%$ ), hydrochloric acid, sodium hydroxide, calcium chloride, acetone, and sodium chloride, all of which were utilised without additional purification. Deionised water ( $18.2 \text{ M}\Omega \cdot \text{cm}$ ) was used to prepare all solutions. Thermo Scientific supplied dialysis tubing with a molecular weight cut-off of 12 kDa. Analytical grade reagents were utilised for all other polysaccharide analysis and adsorption tests.

### 2.2. Extraction and Purification of Sulfated Fucoidan

A modified hot-water extraction process that maximises yield and preserves sulphate groups was used to extract fucoidan from *Undaria pinnatifida*. After being properly cleaned with deionised water to get rid of salts and surface contaminants, the dried seaweed was air-dried, powdered, and then defatted by refluxing in 70% ethanol to get rid of lipids and colours. The pretreatment biomass (50 g) was heated to  $85^\circ\text{C}$  for three hours while being continuously stirred. It was suspended in deionised water at a material-to-solvent ratio of 1:20 (w/v). After cooling and filtering out insoluble residues, the extract was treated with 0.2 M  $\text{CaCl}_2$  to preferentially precipitate alginates. Following centrifugation to remove the alginate fraction, the cleared extract was concentrated under low pressure and ethanol precipitation was applied by gradually adding cooled ethanol to reach a final concentration of 75% (v/v). Centrifugation was used to recover the precipitated polysaccharide, which was then twice cleaned with 70% ethanol and acetone, dissolved in water, and deproteinised using papain enzymatic treatment at  $55^\circ\text{C}$  for four hours. After the enzyme was deactivated by

heating the solution, it was dialysed against deionised water for 72 hours with frequent water changes. Purified sulfated fucoidan powder was obtained by lyophilising the dialysate.

### 2.3. Preparation of Fucoidan Hydrogel (FUC-HG)

Ionic crosslinking was used to create FUC-HG, a stable three-dimensional network appropriate for cadmium adsorption. A homogenous viscous solution was achieved by dissolving purified fucoidan in warm deionised water (4% w/v) and stirring the mixture. The polymer solution was added dropwise to a 2% (w/v)  $\text{CaCl}_2$  solution that was gently agitated. This allowed for the instantaneous creation of gel beads, which were caused by ionic coordination between  $\text{Ca}^{2+}$  and sulphate groups. The resulting hydrogel beads were periodically cleaned with deionised water to get rid of unattached ions after being cured for 24 hours at  $4^\circ\text{C}$  to improve structural stability. For batch adsorption investigations, the hydrogels were crushed to the appropriate particle size after being dried at  $50^\circ\text{C}$ .

### 2.4. Batch Adsorption Experiments

The effectiveness of FUC-HG in removing  $\text{Cd}^{2+}$  at different physicochemical conditions was assessed using Batch Adsorption experiments. 50 mL of  $\text{Cd}^{2+}$  solutions with starting concentrations ranging from 10 to 300 mg/L were mixed with a known mass of hydrogel (usually 20–30 mg). Diluted HCl or NaOH was used to modify the pH of the solutions between 2 and 7 while the suspensions were shaken at 150 rpm in a thermostatic orbital shaker. Depending on the kinetic study design, the contact period ranged from 5 to 240 minutes, and temperature effects were investigated at 25, 35, and  $45^\circ\text{C}$ . Following adsorption, the solutions were filtered, and AAS was used to measure the residual  $\text{Cd}^{2+}$  concentration. Standard mass balance equations were used to compute the removal effectiveness (%) and adsorption capacity ( $q_e$ ).

### 2.5. Isotherm Modelling

Five popular isotherm models the Langmuir, Freundlich, Temkin, Dubinin-Radushkevich

(D-R), and Elovich models were fitted to experimental data in order to clarify the equilibrium adsorption behaviour. The maximum monolayer adsorption capacity ( $q_m$ ), adsorption intensity ( $n$ ), binding constant ( $K^1$ ), surface heterogeneity, and mean free energy of adsorption were all determined using these models. Mechanistic interpretation of surface homogeneity, monolayer versus multilayer adsorption, and the potential energy of interaction between  $Cd^{2+}$  and sulfate-rich functional sites was made possible by the thorough comparison.

### 2.6. Adsorption Kinetics

Time-dependent adsorption studies at an ideal concentration of  $Cd^{2+}$  were used to assess kinetic behaviour. Five kinetic models pseudo-first-order, pseudo-second-order, Elovich, intraparticle diffusion, and Pore Diffusion models were fitted to the acquired  $q_t$  vs. time curves. Nonlinear regression was used to fit each model in order to ascertain the kinetic order, diffusion parameters, sorption intensity, and rate constants. By differentiating between film diffusion, intraparticle transport, chemisorption, and multimechanistic routes that contribute to  $Cd^{2+}$  uptake by the fucoidan hydrogel, the combination of kinetic models allows for a thorough understanding of the governing rate-limiting stages.

### 2.7. Thermodynamic Analysis

To comprehend the viability and energetic nature of  $Cd^{2+}$  adsorption, thermodynamic characteristics were assessed. The van't Hoff equation was utilised to compute changes in Gibbs free energy ( $\Delta G^\circ$ ), enthalpy ( $\Delta H^\circ$ ), and entropy ( $\Delta S^\circ$ ) utilising distribution coefficients ( $K_e$ ) acquired at various temperatures. The spontaneity, endo/exothermic nature, and increased unpredictability related to the adsorption process on the FUC-HG surface were shown by the sign and magnitude of these characteristics.

### 2.8. Reusability and Stability Tests

Adsorption-desorption cycles were used to evaluate the hydrogel's capacity for regeneration. After being desorbed with 0.1 M HCl and cleaned with deionised water

until the pH was neutral, loaded hydrogels were recycled for further cycles under the same circumstances. The hydrogel's structural resilience and the strength of the  $Cd^{2+}$  binding interactions were assessed by measuring the loss in adsorption efficiency and evaluating the stability and reusability across five consecutive cycles.

## 3. Results and Discussion

### 3.1. Influence of pH on Cadmium Uptake and Surface Chemistry

The interaction between  $Cd^{2+}$  ions and the FUC-HG was significantly impacted by the pH of the solution. Protonation of sulphate groups reduced the availability of negatively charged binding sites under extremely acidic circumstances, leading to low absorption [30]. Deprotonation of  $-SO_3^-$  groups boosted the electrostatic attraction towards  $Cd^{2+}$  as pH rose towards the ideal range, resulting in a dramatic increase in adsorption capacity. The creation of cadmium hydroxide species, which decreased the population of free  $Cd^{2+}$  ions available for binding, was thought to be the cause of minor drops in adsorption beyond the ideal threshold. This pH-dependent trend demonstrated the strong pH-responsive binding behaviour of the sulfate-rich fucoidan matrix and the predominance of electrostatic attraction and metal sulfate coordination in  $Cd^{2+}$  adsorption. The hydrogel's potential for practical use under environmental pH ranges characteristic of contaminated water systems was underlined by the well-defined pH window for maximal adsorption.

### 3.2. Effect of Adsorbent Dosage and Surface Accessibility

A progressively higher availability of active functional sites was suggested by a gradual improvement in removal efficiency with increasing hydrogel dosage. However, because of unsaturated binding sites, particle aggregation, and lower driving force per unit mass, the equilibrium adsorption capacity ( $q_e$ ) dropped at higher dosages [31]. Biopolymer-based hydrogels frequently exhibit this behaviour, where high swelling capacity causes polymer domains to overlap

at high doses, limiting ion migration into deeper matrix regions [32]. The plateauing pattern indicated that the FUC-HG has both accessible surface sites and a highly porous interior structure that facilitates efficient diffusion of Cd<sup>2+</sup> under optimal dose. These findings emphasise how crucial dosage control is for maximising cost effectiveness in real-world water treatment applications rather than for boosting intrinsic capability.

### 3.3. Effect of Initial Cadmium Concentration and Mass Transfer Driving Force

Because of the large ratio of accessible binding sites to Cd<sup>2+</sup> ions, the hydrogel quickly reached equilibrium at lower starting concentrations. The adsorption curve changed from a high-affinity region to a saturation-driven plateau as concentration rose, indicating the active sulphate groups' increasing occupied. Increased mass transfer rate and quicker diffusion through the hydrogel matrix were made possible by higher driving force at higher Cd<sup>2+</sup> levels. But as the hydrogel gets closer to its natural loading capacity, the final saturation showed that the adsorption mechanism changes from site-rich to site-limited circumstances. The behaviour verified the balance between intraparticle transport and exterior film diffusion, which controls the overall uptake process, as well as the strong affinity between Cd<sup>2+</sup> and the fucoidan network.

#### 3.3.1. Adsorption isotherms

The performance evaluation of any sorbent is purely based on its ability to uptake the maximum concentration of heavy metals from aqueous solutions. Therefore, the batch experimental data in Table. 1. obtained from the effect of the initial concentration of Cd(II) on sorption capacity of the sorbent was applied to the linear forms of Freundlich, Langmuir, D-R, and Elovich, and Temkin model equations to know about the maximum sorption capacity of FUC-HG and mechanism of sorption phenomenon. Also, the physisorption or chemisorption nature of the sorption process was predicted from these isotherms.

#### 3.3.1.1. Freundlich Isotherm

The Freundlich isotherm analysis (log q<sub>e</sub> vs. log C<sub>e</sub>, R<sup>2</sup> = 0.9441) indicates the heterogeneous surface adsorption behavior of FUC-HG, in which several binding sites with different affinities are involved in the uptake of ions ~50 mg/g. This strong fit suggests that the hydrogel's uptake of metal ions is effectively captured by the isotherm. The Freundlich relationship is mathematically given by

$$q_e = K_F C_e^{1/n} \quad (\text{Eq. 1})$$

in which q<sub>e</sub> denotes the amount of solute per unit mass of adsorbent at equilibrium, C<sub>e</sub> is the corresponding equilibrium concentration of the ions. K<sub>F</sub> represents a capacity-related constant, and 1/n provides insight into the degree of surface site heterogeneity. The Freundlich equation in linear form is:

$$\log q_e = \log K_F + \frac{1}{n} \log C_e \quad (\text{Eq. 2})$$

The slope (1/n = 0.7233), as seen in Fig. 1A, is between 0 and 1, indicating favourable adsorption and notable surface heterogeneity. The fucoidan network's abundance of sulfated groups (-SO<sub>3</sub><sup>-</sup>) and remaining hydroxyl functionalities, which provide adsorptive sites with varying energy levels and capabilities for Cd<sup>2+</sup> binding, are the cause of this variability. These high-affinity surface sites facilitate quick and effective uptake at lower metal ion concentrations; as concentration rises, these sites gradually get occupied, resulting in multilayer accumulation on lower-energy areas of the polymeric matrix. As a result, FUC-HG functions as a non-uniform, heterogeneous sorbent that can hold Cd<sup>2+</sup> by a variety of interactions, including complexation, ion exchange, and electrostatic attraction. As a result, the FUC-HG varied chemical activity permits strong adsorption over a broad concentration range, indicating its promise as a flexible and effective bioadsorbent for wastewater treatment.

#### 3.3.1.2. Langmuir Isotherm

The Langmuir isotherm model (C<sub>e</sub>/q<sub>e</sub> vs C<sub>e</sub>, R<sup>2</sup> = 0.8792) confirms that it operates by

monolayer adsorption capacity with FUC-HG which absorbed metal ions from the solution to reach finite binding sites evenly distributed throughout the surface shown in Fig. 1B. The Langmuir equation is

$$q_e = \frac{Q_{\max} b C_e}{1 + b C_e} \quad (\text{Eq. 3})$$

where  $q_e$  is the amount of adsorbate adsorbed at equilibrium ( $\text{mg g}^{-1}$ ),  $Q_{\max}$  is the maximum monolayer adsorption capacity ( $\text{mg g}^{-1}$ ),  $b$  is the Langmuir constant related to the affinity of binding sites ( $\text{L mg}^{-1}$ ),  $C_e$  is the equilibrium concentration of adsorbate in

solution ( $\text{mg L}^{-1}$ ). The linear form of Langmuir equation is

$$\frac{C_e}{q_e} = \frac{1}{Q_{\max} \times b} + \frac{C_e}{Q_{\max}} \quad (\text{Eq. 4})$$

The Langmuir isotherm's positive slope and distinct intercept indicate that each adsorption site on FUC-HG holds a single  $\text{Cd}^{2+}$  ion, which is compatible with the idea of monolayer surface coverage. This behaviour suggests the existence of spatially well-defined and energetically equivalent binding sites in the hydrogel matrix, which are mainly linked to the hydroxyl and sulfated ( $-\text{SO}_3^-$ ) functional groups present in the fucoidan backbone. Through ion-exchange interactions and electrostatic attraction, these functional moieties offer particular coordination conditions that promote selective  $\text{Cd}^{2+}$  binding.

Although the Freundlich model emphasises surface heterogeneity and multilayer adsorption behaviour, the Langmuir model's strong applicability shows that uniform, site-specific interactions account for a sizable portion of  $\text{Cd}^{2+}$  uptake. A dual adsorption mechanism in FUC-HG, comprising both monolayer adsorption on high-energy, homogeneous sites and multilayer accumulation on heterogeneous portions of the hydrogel network, is indicated by the coexistence of Freundlich and Langmuir properties. By expanding the operational concentration range and improving ion-exchange efficiency, this coupled adsorption

behaviour allows FUC-HG to remove  $\text{Cd}^{2+}$  ions from aqueous environments in a highly effective and selective manner.

### 3.3.1.3. Dubinin–Radushkevich (D–R) isotherm

From the D–R isotherm plot ( $\ln q_e$  vs.  $\varepsilon^2$ ,  $R^2 = 0.9878$ ) in Fig. 1C, it can be understood that the adsorption of heavy metal ions by FUC-HG is conditioned best by this model and a chemisorption interception controlled process takes place. The D-R equation is given by

$$q_e = X_m e^{-\beta \varepsilon^2} \quad (\text{Eq. 5})$$

Where  $q_e$  is the equilibrium adsorption capacity ( $\text{mg g}^{-1}$ ),  $X_m$  is the theoretical saturation capacity ( $\text{mg g}^{-1}$ ),  $\beta$  is the D-R constant ( $\text{mol}^2 \text{J}^{-2}$ ), related to adsorption energy,  $\varepsilon$  is the Polanyi potential calculated through  $\varepsilon = RT \ln(1 + 1/C_e)$ . The linear form of D-R equation is

$$\ln q_e = \ln X_m - \beta \varepsilon^2 \quad (\text{Eq. 6})$$

$$\varepsilon^2 = RT \ln \left( 1 + \frac{1}{C_e} \right) \quad (\text{Eq. 7})$$

$$E = \frac{1}{\sqrt{-2\beta}} \quad (\text{Eq. 8})$$

The computed mean adsorption energy ( $E > 8 \text{ kJ mol}^{-1}$ ) suggests that chemical adsorption, rather than weak physical interactions like van der Waals forces [32], is the primary mechanism of  $\text{Cd}^{2+}$  uptake by FUC-HG. The presence of high-affinity binding sites on the hydrogel surface that interact with  $\text{Cd}^{2+}$  ions selectively is confirmed by the size of the adsorption energy.

The predominance of chemisorption indicates that ion-exchange and coordination mechanisms, wherein sulfated ( $-\text{SO}_3^-$ ) and hydroxyl ( $-\text{OH}$ ) functional groups within the fucoidan backbone create strong ionic or coordination interactions with  $\text{Cd}^{2+}$  ions, are the main mechanisms by which FUC-HG operates. The metal ions in the hydrogel network are stabilised as a result of these interactions. The high adsorption efficiency,

selectivity, and specificity of FUC-HG towards Cd<sup>2+</sup> are explained by the frequency of such chemically driven interactions, highlighting its great promise as an efficient bioadsorbent for the removal of hazardous cadmium ions from contaminated wastewater.

#### 3.3.1.4. Elovich Model

The adsorption behaviour of Cd<sup>2+</sup> ions onto FUC-HG can be better understood using the Elovich kinetic model (Fig. 1D), especially in situations where chemically controlled processes predominate. Because the fucoidan hydrogel has a large number of sulfated (–SO<sub>3</sub><sup>–</sup>) and hydroxyl (–OH) functional groups dispersed throughout the polymeric network, this model is well suited for explaining adsorption on energetically heterogeneous surfaces. Strong chemisorptive binding rather than straightforward physical adsorption is the outcome of these multifunctional sites' active participation in ion-exchange and coordination interactions with Cd<sup>2+</sup> ions.

The linear form of Elovich equation is

$$\ln \frac{q_e}{C_e} = \ln K_E Q_{\max} - \frac{q_e}{Q_{\max}} \quad (\text{Eq. 9})$$

A dual-stage adsorption mechanism for Cd<sup>2+</sup> uptake is suggested by the Elovich kinetic behaviour of FUC-HG. Due to the large number of easily accessible high-energy binding sites on the hydrogel surface, where Cd<sup>2+</sup> ions are swiftly immobilised via monolayer ion-exchange and coordination contacts, adsorption proceeds quickly in the first stage [33]. This rapid uptake is a result of the fucoidan network's sulfated and hydroxyl functional groups having a significant affinity for Cd<sup>2+</sup> ions and low surface coverage.

Diffusion-controlled multilayer adsorption within the porous hydrogel matrix dominates the second stage, which is indicated by the rate steadily declining as adsorption advances. During this stage, Cd<sup>2+</sup> ions go into the interior of FUC-HG and engage in stronger chemisorption interactions with functional groups. The heterogeneous and

chemically controlled nature of Cd<sup>2+</sup> adsorption is highlighted by the coexistence of rapid surface binding and slower intraparticle diffusion, indicating that FUC-HG functions effectively over a broad concentration range a crucial characteristic for realistic wastewater treatment applications [34].

#### 3.3.1.5. Temkin Isotherm

The Temkin isotherm characterizes systems where the interaction energy between solute and substrate diminishes uniformly as surface coverage rises, thereby highlighting the importance of solute - substrate cooperative interactions [35]. The linear  $q_e$  versus  $\ln C_e$  relationship observed for FUC-HG ( $R^2 = 0.9682$ ) corroborates this model and indicates that solute-substrate interactions materially influence the uptake. The mathematical formulation is given by

$$q_e = \frac{\kappa T}{b} \ln(K C_e) \quad (\text{Eq. 10})$$

where R is the universal gas constant, T is absolute temperature, K<sub>t</sub> is the Temkin affinity constant, and b is linked to the adsorption heat. The linear form of temkin equation is

$$q_e = B \ln A + B \ln C_e \quad (\text{Eq. 11})$$

The effective heat of adsorption during Cd<sup>2+</sup> absorption by FUC-HG is reflected in the rising trend of the  $q_e$  versus  $\ln C_e$  plot (Fig. 1E). Due to the sequential occupation of high-energy binding sites and electrostatic repulsion among adsorbed ions, this behaviour suggests that the adsorption energy gradually reduces with increasing Cd<sup>2+</sup> concentration. Cd<sup>2+</sup> ions first preferentially occupy energetically favourable sulfate-rich locations on the hydrogel surface; as these sites get saturated, adsorption moves to lower-energy areas of the hydrogel matrix, which lowers the incremental adsorption strength.

This kind of behaviour is typical of sulfated biopolymer hydrogels, where coordination with functional groups, ion-exchange interactions, and electrostatic attraction all

work together to control Cd<sup>2+</sup> binding instead of just weak physical forces [35]. The success of FUC-HG as a high-performance ion-exchange material for cadmium removal

from aqueous systems is confirmed by the progressive filling of sites with decreasing adsorption energy, which supports a multilayer adsorption mechanism

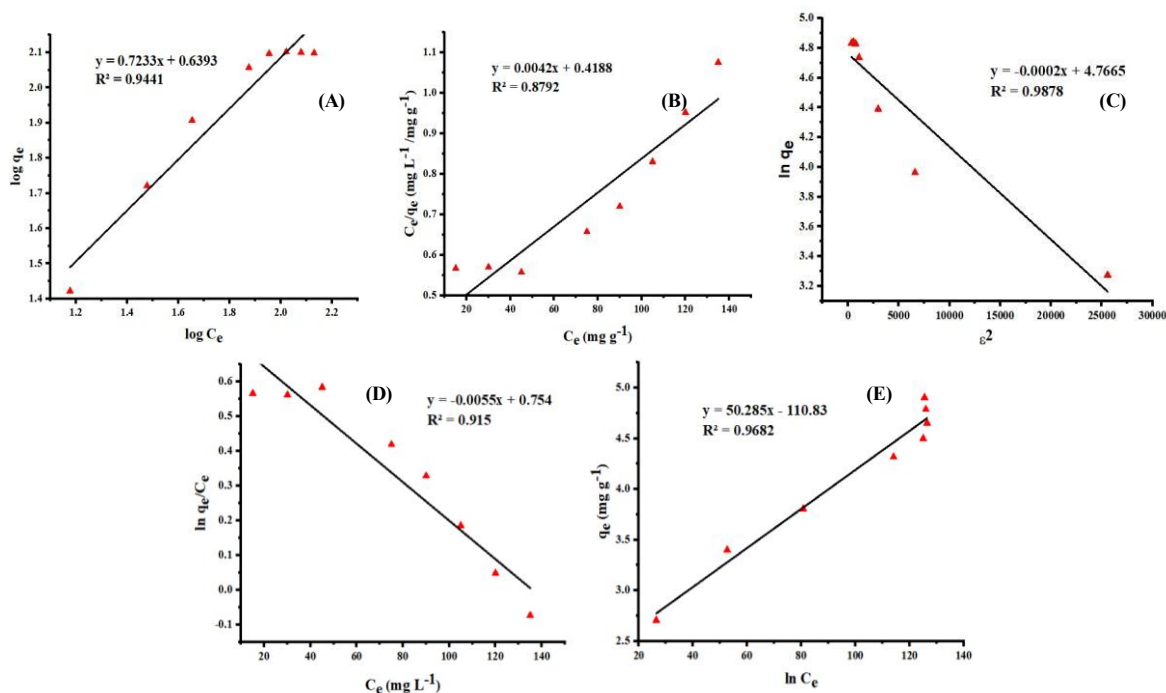


**Fig. 1.** Adsorption isotherms of Cd<sup>2+</sup> onto FUC-HG. (A) Freundlich Isotherm, (B) Langmuir Isotherm, (C) Dubinin–Radushkevich Isotherm, (D) Elovich Model, and (E) Temkin Isotherm

**Table. 1.** The isothermal parameters of linear forms of Freundlich, Langmuir, Dubinin-Radushkevich, Elovich, and Temkin models for the Cd<sup>2+</sup> uptake by FUC-HG.

Experimental	$q_e$ (mgg <sup>-1</sup> )	126.4381
Freundlich	$K_F$	4.358127
	$N$	1.382607
	$R^2$	0.9441
Langmuir	$Q_{max}$ (mg g <sup>-1</sup> )	238.2801
	$b$ (mg L <sup>-1</sup> )	0.010021
	$R_L$	2.352858
	$R^2$	0.8792
D-R	$X_m=Q_{max}$ (mg g <sup>-1</sup> )	116.9396
	$\beta$ (kJ <sup>2</sup> /mol <sup>2</sup> )	-2.52201E-08
	$E$	4452.574
	$R^2$	0.9878
Elovich	$Q_{max}$ (mg g <sup>-1</sup> )	201.8114
	$KE(Lmg^{-1})$	1.00002
	$R^2$	0.915
Temkin	$B$	50.2847
	$A$	0.110347
	$b_T(J mol^{-1})$	49.27089
	$R^2$	0.9682

### 3.3.2. Kinetic Models

The appraisal of sorption kinetics is one of the key factors to evaluate the rate at which sorbent can uptake the highest amounts of heavy metals from the parent contaminated systems. The kinetic study of the sorption process gives direct insight into reaction pathways. Thereby, information about the evaluation of the mechanism of bonding could be explained by fitting sorption data of contact time experiments to the linear forms of pseudo-first-order, pseudo-second-order, intraparticle diffusion, pore diffusion, and Elovich kinetics models [36] as shown in Table.2.

#### 3.3.2.1. Pseudo-first-order model

The pseudo-first-order (PFO) model is also founded on the supposition that rate of adsorption is proportional to the sites available for adsorption and usually suitable for physisorbed species. The kinetics equation for pseudo-first order in linear form is

$$\log(q_e - q_t) = \log q_e - \frac{k}{2.303} t \quad (\text{Eq. 12})$$

The pseudo-first-order (PFO) kinetic model (Fig. 2A) for FUC-HG showed a significant difference between estimated ( $q_{e,\text{cal}}$ ) and experimental ( $q_{e,\text{exp}}$ ) adsorption capabilities, as well as a low regression coefficient ( $R^2 = 0.4099$ ).  $\text{Cd}^{2+}$  adsorption does not follow a straightforward physisorption-controlled mechanism controlled by surface film diffusion, as evidenced by the divergence from linearity and the non-uniform distribution of residuals. Rather, first-order kinetics is insufficient to explain the quick initial uptake shown in experiments.

The chemical structure of FUC-HG, which has a high density of active sulfated ( $-\text{SO}_3^-$ ) and hydroxyl ( $-\text{OH}$ ) functional groups capable of significant ion-exchange and coordination interactions with  $\text{Cd}^{2+}$  ions, is compatible with the PFO model's restricted applicability. Adsorption occurs by a mixture of surface binding, intraparticle diffusion, and chemisorption since the hydrogel matrix is porous and extremely swellable. Therefore, the poor agreement with the PFO

model indicates that strong site-specific chemical interactions rather than weak physical adsorption dominate  $\text{Cd}^{2+}$  removal by FUC-HG, supporting the appropriateness of higher-order kinetic models to describe the system.

#### 3.3.2.2. Pseudo-second-order model

Heavy metal ions adsorption onto FUC-HG showed a pseudo-second-order (PSO) model and an excellent fit as indicated by the correlation coefficient ( $R^2 = 0.9876$ ) in Fig. 2B. The model's linear form is written like this

$$\frac{t}{q_t} = \frac{1}{k_2 q_e^2} + \frac{t}{q_e} \quad (\text{Eq. 13})$$

In this equation,  $q_t$  is the amount of metal ions grabbed at time  $t$  in mg/g,  $q_e$  is the amount at the end in mg/g, and  $k_2$  is the rate constant in g/mg/min.

According to the pseudo-second-order (PSO) kinetic model, chemisorption involving electron sharing or exchange between the adsorbent and adsorbate controls the rate-limiting step of adsorption.  $\text{Cd}^{2+}$  adsorption onto FUC-HG proceeds primarily through a chemically regulated mechanism rather than simple physical adsorption, as demonstrated by the excellent agreement between the experimental data and the PSO model. This robust model fit further demonstrates that particular interactions at the active binding sites, rather than just diffusion or external mass transfer, control the adsorption kinetics. The functional chemistry of the fucoidan hydrogel is intimately related to the applicability of the PSO model from a mechanistic standpoint. Sulfated ( $-\text{SO}_3^-$ ) and hydroxyl ( $-\text{OH}$ ) groups abound in the FUC-HG matrix, offering numerous coordination sites that can bind  $\text{Cd}^{2+}$  ions via ion exchange and complexation processes. In the three-dimensional hydrogel network, these functional groups serve as chemically active anchors that facilitate quick initial absorption and stabilisation once equilibrium is reached. Therefore, the dominance of PSO kinetics demonstrates the efficacy of FUC-HG as a strong and chemically active bioadsorbent for wastewater purification and reveals that

Cd<sup>2+</sup> removal by FUC-HG is controlled by strong, site-specific chemical interactions.

### 3.3.2.3. Intraparticle diffusion model

The intraparticle diffusion model was also employed for a deeper comprehension of the rate-limiting step in Cd<sup>2+</sup> adsorption onto the FUC-HG. To find out which step limited how quickly heavy metal ions stick to FUC-HG, we used the intraparticle diffusion model first suggested by Weber and Morris:

$$q_t = k_{idm} t^{1/2} + C \quad (Eq. 14)$$

In this formula,  $k_{idm}$  (mg g<sup>-1</sup> min<sup>-1/2</sup>) is the rate constant for diffusion into the particle, and  $C$  (mg g<sup>-1</sup>) is the intercept of the line, which tells us about the boundary layer effect around the particle.

Cd<sup>2+</sup> adsorption onto FUC-HG occurs via a multistep mechanism, as seen by the plot of  $q_t$  versus  $t^{1/2}$  (Fig. 2C), which shows a quick initial absorption followed by a progressive plateau. Surface adsorption and boundary layer diffusion, where numerous and easily accessible sulfated binding sites on the hydrogel surface facilitate quick Cd<sup>2+</sup> uptake, are responsible for the initial stage's rapid adsorption rate. A slower phase controlled by intraparticle diffusion ensues, during which Cd<sup>2+</sup> ions move into the hydrogel network's interior pores and swelling domains.

The diffusion plot's nonlinearity and the lack of a straight line through the origin show that exterior film diffusion also plays a major role in the adsorption process and that intraparticle diffusion is not the only rate-limiting phase. When equilibrium is reached, the majority of active sites are occupied and additional Cd<sup>2+</sup> transport into the hydrogel matrix is restricted. This is reflected in the observed plateau. Overall, these findings highlight the efficacy of the porous, sulfated hydrogel structure for effective heavy-metal removal from aqueous systems by showing that Cd<sup>2+</sup> adsorption by FUC-HG is regulated by a combined mechanism involving surface adsorption, pore diffusion, and boundary layer resistance.

### 3.3.2.4. Pore diffusion

Bangham's equation helps us see how much pore diffusion affects how heavy metal ions stick to FUC-HG. The equation looks like

this

$$q_t = \ln k_B + \alpha_B \ln t \quad (Eq. 15)$$

Where  $k_B$  (m mg<sup>-1</sup>) denoted the Bangham Constant whose value described the sorption maxima,  $\alpha_B$ , is constant for pore diffusion whose value should be less than unity, ( $q_t/q_\infty = 1$ ) is the film diffusion constant (min<sup>-1</sup>).

The Weber–Morris pore diffusion model was used to analyse the adsorption data in order to examine the role of intraparticle transport in Cd<sup>2+</sup> uptake [37]. The plot of  $\ln q_t$  versus  $\ln t$  revealed a roughly linear connection ( $R^2 = 0.8628$ ), suggesting that pore diffusion is important for the adsorption process in Fig. 2D. Nevertheless, the line did not cross the origin, indicating that surface adsorption and boundary layer resistance both affect the overall kinetics, indicating that adsorption is not only controlled by pore diffusion.

The nonzero intercept measures the initial resistance at the hydrogel solution interface, whereas the slope of the Weber–Morris plot indicates the rate of ion transport into the hydrogel pores. These findings lend credence to a progressive adsorption mechanism in which Cd<sup>2+</sup> ions quickly attach to accessible surface sites, diffuse through the polymer's boundary layer, and then delve further into the internal pore network. The great efficacy of FUC-HG in sequestering Cd<sup>2+</sup> ions from aqueous solutions can be explained by this layered adsorption behaviour, which is typical of biopolymer-based hydrogels and combines surface ion exchange with intraparticle movement.

### 3.3.2.5. Elovich model

Fig. 2E. shows how well the Elovich kinetic model describes metal-ion adsorption on FUC-HG. This model is ideal when adsorption occurs on surfaces with varying binding energies and is primarily controlled by chemical attachment. The Elovich model is given by

$$q_t = \frac{1}{\beta} \ln(\alpha\beta) + \frac{1}{\beta} \ln t \quad (Eq. 16)$$

$\alpha$  (mg g<sup>-1</sup> min<sup>-1</sup>) is the initial adsorption speed, while  $\beta$  (g mg<sup>-1</sup>) relates to how fully the surface can fill and how much energy is needed for the adsorption to occur. The

kinetics of  $\text{Cd}^{2+}$  adsorption on FUC-HG were assessed using the Elovich model, which produced a linear  $t/q_t$  vs  $\ln t$  plot with a significant correlation coefficient ( $R^2=0.8887$ ). This suggests that the hydrogel's surface is heterogeneous and contains active binding sites with different energies. An examination of the Elovich characteristics reveals a low desorption constant ( $\beta$ ), indicating that ions remain firmly fixed by chemical interactions after adsorption, and a high initial adsorption rate ( $\alpha$ ), indicating the quantity of easily accessible sites for quick  $\text{Cd}^{2+}$  uptake.

The Elovich model's better fit than the pore diffusion model emphasises that surface reactions and chemisorption, rather than intraparticle diffusion, are the main factors influencing  $\text{Cd}^{2+}$  uptake. Strong ion-exchange and coordination contacts are facilitated by functional groups within FUC-HG, especially hydroxyl ( $-\text{OH}$ ) and sulfated ( $-\text{SO}_3^-$ ) moieties, which help remove  $\text{Cd}^{2+}$  ions effectively and selectively. These findings show that FUC-HG is an efficient bioadsorbent for wastewater treatment due to its highly reactive and diverse surface.

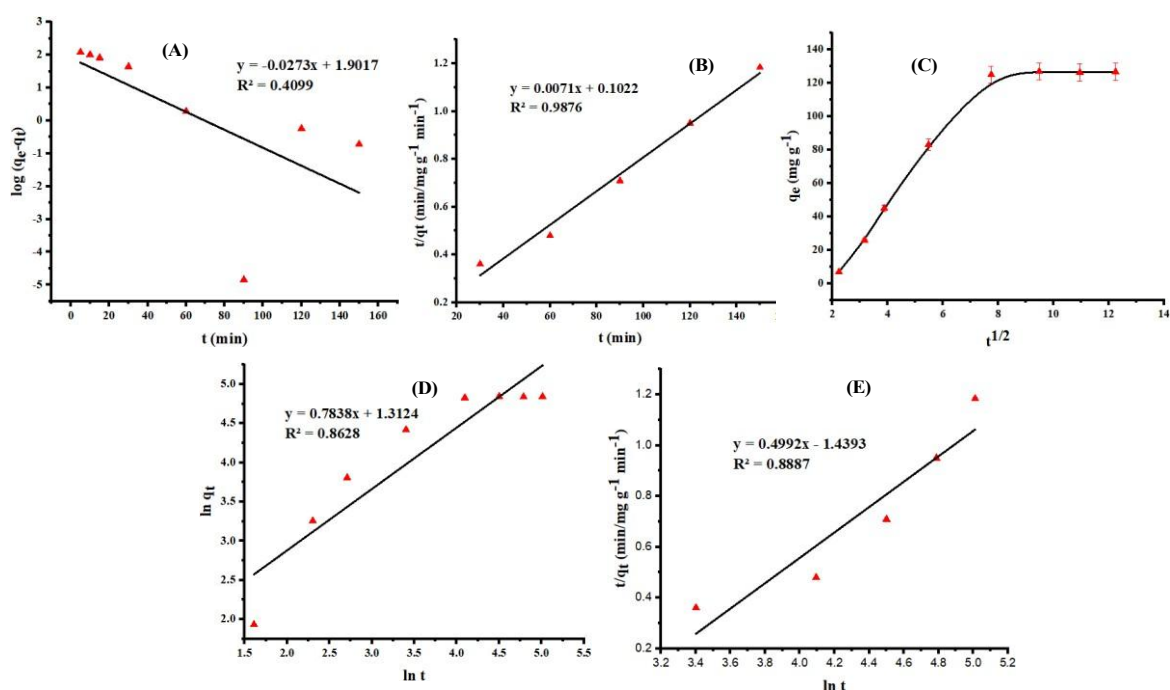


**Fig. 2.** Kinetic Models for adsorption of  $\text{Cd}^{2+}$  onto FUC-HG. (A) Pseudo-First-Order kinetics, (B) Pseudo-Second-Order Kinetics, (C) Intraparticle Diffusion model, (D) Pore diffusion, and (E) Elovich Model

**Table 2.** The kinetics parameters of linear forms of pseudo-first-order, pseudo-second-order, intraparticle diffusion, pore diffusion, and Elovich models for the Cd(II) uptake by FUC-HG.

Experimental		$q_e$ (mgg <sup>-1</sup> )	126.9143
Pseudo-first-order		$q_e$ (mg g <sup>-1</sup> )	6.697203
		$k_1$ (g mg <sup>-1</sup> min <sup>-1</sup> )	0.062871
		$R^2$	0.4099
Pseudo-second-order		$q_e$ (mg g <sup>-1</sup> )	210.53
		$k_2$ (g mg <sup>-1</sup> min <sup>-1</sup> )	2.20891E-05
		$R^2$	0.9876
Intra-particle diffusion model	Stage I	$K_{id}$ (mg g <sup>-1</sup> min <sup>-0.5</sup> )	21.74002
		$I$ (mg g <sup>-1</sup> )	-40.6063
		$R^2$	0.9958
	Stage II	$K_{id}$ (mg g <sup>-1</sup> min <sup>-0.5</sup> )	0.320613
		$I$ (mg g <sup>-1</sup> )	123.0066
		$R^2$	0.5229
Pore Diffusion		$K_\beta$	20.5288
		$\alpha_\beta$	0.783823
		$R^2$	0.8628
Elovich isotherm		$\alpha$ (mg (g min) <sup>-1</sup> gmg <sup>-1</sup> )	0.02794
		$\beta$ (mg (g min) <sup>-1</sup> gmg <sup>-1</sup> )	2.003092
		$R^2$	0.8887

### 3.4. Effect of Temperature on Cd<sup>2+</sup> Uptake Beyond Thermodynamics

The experimental temperature-dependent performance gave additional mechanistic knowledge, even though thermodynamic parameters shed light on spontaneity and energetic nature. Raising the temperature enhanced intramolecular mobility in the hydrogel matrix, lowering diffusion resistance and increasing the accessibility of sulphate groups [38]. Wider diffusion channels were produced by the increased swelling seen at higher temperatures, which improved the penetration of hydrated Cd<sup>2+</sup> ions. However, very high temperatures caused slight reductions in capacity, which could be explained by a partial rupture of the

three-dimensional network of the hydrogel. The idea that the fucoidan hydrogel functions through a dual mechanism involving both surface binding and interior matrix diffusion is supported by this temperature-governed swelling diffusion connection.

#### 3.4.1. Sorption Thermodynamics

For better understanding of the feasibility and the nature of the adsorption

phenomenon, the thermodynamic parameters were determined by the temperature dependence of metal ion uptake on the FUC-HG in Table. 3. The values of these factors were calculated by using these equations [39].

The  $\Delta G^\circ$  is associated with the equilibrium constant ( $K_c$ ) and was calculated using the given below Eq. 17. The  $\Delta H^\circ$  and  $\Delta S^\circ$  were calculated using Vant's Hoff isotherm (Eq. 19).

$$\Delta G^\circ = -RT \ln K_c \quad (\text{Eq. 17})$$

$$K_c = \frac{q_e}{C_e} \quad (\text{Eq. 18})$$

$$\ln K_c = \frac{\Delta S^\circ}{R} - \frac{\Delta H^\circ}{RT} \quad (\text{Eq. 19})$$

A spontaneous and endothermic process is shown by the thermodynamic characteristics of Cd<sup>2+</sup> adsorption onto FUC-HG. While the positive  $\Delta H^\circ$  indicates the endothermic nature, the negative  $\Delta G^\circ$  values validate the spontaneity of adsorption, indicating that higher temperatures improve Cd<sup>2+</sup> transport into the hydrogel matrix because of greater

molecular mobility and stronger contacts with active sites. The displacement of solvated water molecules during ion binding is probably the cause of the positive  $\Delta S^\circ$ , which shows an increase in randomness at the solid solution interface. These findings

support the kinetic analysis and demonstrate the dominance of chemisorption. Overall, the thermodynamic analysis shows that FUC-HG is a stable and effective bioadsorbent for the removal of  $\text{Cd}^{2+}$  that may function well in a variety of environmental settings.

**Table 3.** Thermodynamic parameters of sorption of Cd(II) onto FUC-HG.

Thermodynamic parameter	$\Delta S^\circ$ (J mol <sup>-1</sup> K <sup>-1</sup> )	98.6
	$\Delta H^\circ$ (kJ mol <sup>-1</sup> )	24.8
	$\Delta G^\circ$ (kJ mol <sup>-1</sup> )	-4.58

### 3.5. Influence of Ionic Strength and Competing Ions

The uptake of  $\text{Cd}^{2+}$  was greatly impacted by the presence of background electrolytes, especially at higher ionic strengths where charge shielding decreased the effective electrostatic interaction between  $\text{Cd}^{2+}$  and the negatively charged sulphate groups. By directly competing for sulphate binding sites, divalent ions like  $\text{Ca}^{2+}$  or  $\text{Mg}^{2+}$  imposed more interference than monovalent cations like  $\text{Na}^+$ . However, the hydrogel maintained a significant amount of its adsorption capability even at high ionic strength, indicating the specificity of the sulphate cadmium interaction. This competitive performance suggests that the fucoidan hydrogel may perform well in actual wastewater matrices with mixed ions [40].

### 3.6. Proposed Adsorption Mechanism at the Molecular Level

Metal ligand chelation, intraparticle diffusion, and electrostatic attraction work in concert to control the adsorption of  $\text{Cd}^{2+}$  onto the FUC-HG. As the main binding sites, the sulphate groups ( $-\text{SO}_3^-$ ) create persistent ionic or coordinate contacts with  $\text{Cd}^{2+}$  ions. In the hydrogel network, secondary contributions come from hydroxyl groups that offer extra coordination sites, forming bidentate or multidentate complexes [41].  $\text{Cd}^{2+}$  is transported through interconnected holes in the swelling hydrogel matrix, where interactions with internal sulphate domains improve overall uptake. The strong affinity shown in experiments is explained by this hierarchical binding design, which also verifies that fucoidan functions as a naturally

occurring ligand for metal ions because of its high degree of sulfation.

### 3.7. Structural Stability and Integrity of the Hydrogel During Adsorption

The hydrogel showed its resilience in aqueous environments by retaining its structural cohesiveness without appreciable fragmentation or disintegration across several adsorption cycles. Even when competing  $\text{Cd}^{2+}$  ions were present, the strong ionic crosslinking between fucoidan chains and  $\text{Ca}^{2+}$  maintained structural robustness. Rather than physical degradation, partial desorption and progressive occupation of deep matrix sites were found to be the main causes of minor reductions in adsorption capacity with repeated usage. The hydrogel's capability for scalable wastewater remediation was reinforced by the retained morphology and little loss of functional groups, which demonstrated the hydrogel's capacity to function consistently in repeated treatment cycles.

### 3.8. Comparative Performance Perspective with Natural and Synthetic Adsorbents

Even though FUC-HG was the study's main focus, its performance value becomes more apparent when compared to other adsorbents. Because of its high sulphate content, which offers stronger electrostatic and coordination interactions, the FUC-HG showed greater attraction towards  $\text{Cd}^{2+}$  when compared to traditional biopolymers like chitosan, alginate, or pectin. Fucoidan is a more sustainable substitute for synthetic polymeric resins, which are effective but can require complicated manufacture and raise

environmental issues. FUC-HG is a sophisticated bioadsorbent that may satisfy the needs of modern water treatment technologies because of its high Cd<sup>2+</sup> absorption capacity, selectivity in the presence of competing ions, ease of regeneration, and biodegradability.

#### 4. Conclusion

This work shows that FUC-HG, which is made from *Undaria pinnatifida*, is a selective and efficient bioadsorbent for removing Cd<sup>2+</sup> from aqueous solutions. While kinetic analysis matched the pseudo-second-order model ( $R^2 = 0.9876$ ), confirming that chemisorption is the major rate-limiting process, equilibrium adsorption data were best represented by the Freundlich isotherm ( $R^2 = 0.9441$ ), indicating multilayer adsorption on a heterogeneous surface. The adsorption process is spontaneous, endothermic, and entropy-driven ( $\Delta G^\circ < 0$ ,  $\Delta H^\circ > 0$ ,  $\Delta S^\circ > 0$ ), according to thermodynamic analysis, which is in line with the chemisorption mechanism seen in comparable polysaccharide-based hydrogels documented in the literature. The hydrogel's promise for sustainable water treatment was highlighted by its outstanding stability and reusability, as well as its ability to remove Cd<sup>2+</sup> efficiently across several cycles. FUC-HG is a potential material for heavy metal cleanup due to its high adsorption capacity (~50 mg/g), selective ion binding, and chemical resistance. In keeping with other published research on polysaccharide-based bioadsorbents, our findings indicate possible relevance in industrial wastewater treatment, including metal-contaminated effluents from electroplating or mining activities, even if the current results are at the laboratory scale. All things considered, FUC-HG is an economical, eco-friendly, and effective bioadsorbent for the targeted elimination of hazardous heavy metal ions, supporting the mounting evidence that sulfated polysaccharide hydrogels are workable options for water purification.

#### REFERENCES

- [1] Abbas, A., Hussain, M.A., Sher, M., Abbas, N.S. and Ali, M., 2017. Modified hydroxyethylcellulose: a regenerable super-sorbent for Cd<sup>2+</sup> uptake from spiked high-hardness groundwater. *Cellulose Chemistry and Technology*, 51, 167-174.
- [2] Irfan, M.I., Sadiq, M., Zohra, L., Siddique, A.B., Yousaf, M., Rubab, M., Urooj, K., Aziz, A., Ali, H., Fatima, M. and Amin, H.M., 2024. Chemical modification of *Pinus walliichiana* sawdust: Application in membrane system for efficient purification of groundwater containing Cd (II) and Ni (II). *Journal of Water Process Engineering*, 68, 106337.
- [3] Abbas, A., Hussain, M.A., Sher, M., Hussain, S.Z. and Hussain, I., 2017. Evaluation of chemically modified polysaccharide pullulan as an efficient and regenerable supersorbent for heavy metal ions uptake from single and multiple metal ion systems. *Desalination and Water Treatment*, 78, 241-252.
- [4] Lodhi, B.A., Abbas, A., Hussain, M.A., Hussain, S.Z., Sher, M. and Hussain, I., 2019. Design, characterization and appraisal of chemically modified polysaccharide based mucilage from *Ocimum basilicum* (basil) seeds for the removal of Cd (II) from spiked high-hardness ground water. *Journal of Molecular Liquids*, 274, 15-24.
- [5] Ali, A., Akram, A., Bakar, M.A., Amin, H.M., Zohra, L., Abbas, A., Sher, M., Hussain, M.A., Haseeb, M.T. and Imran, M., 2025. A model batch and column study for Cd (II) uptake using citric acid cross-linked *Salvia spinosa* hydrogel: Optimization through Box-Behnken design. *Journal of Industrial and Engineering Chemistry*, 151, 746-761.
- [6] Hussain, A., Fatima, S., Abbas, A., Ali, A., Amin, M., Muhammad, G. and Sher, M., 2023. Removal of Cr (III)

- and Ni (II) from aqueous solution using a mixed cellulose ether-ester hydroxyethylcellulose adipate. *Desalination and Water Treatment*, 283, 153-163.
- [7] Hussain, M.A., Gul, S., Abbas, A., Ali, A. and Alotaibi, N.F., 2021. Chemically modified rhamnogalacturonans from linseed: a supersorbent for Cd<sup>2+</sup> and Pb<sup>2+</sup> uptake from aqueous solution. *Desalination and Water Treatment*, 221, 163-175.
- [8] Shehzad, M.K., Ali, A., Qasim, S., Mumtaz, A., Hussain, M.A., Fawy, K.F., Nishan, U., Azhar, I., Abbas, M.A. and Abba, A., 2025. Sustainable remediation of cadmium using succinate-functionalized glucoxytan from chia (*Salvia hispanica*) seeds hydrogel. *Journal of Industrial and Engineering Chemistry*. <https://doi.org/10.1016/j.jiec.2025.10.034>.
- [9] Ali, A., Haseeb, M.T., Hussain, M.A., Tulain, U.R., Muhammad, G., Azhar, I., Hussain, S.Z., Hussain, I. and Ahmad, N., 2023. A pH responsive and superporous biocomposite hydrogel of *Salvia spinosa* polysaccharide-co-methacrylic acid for intelligent drug delivery. *RSC Advances*, 13(8), 4932-4948.
- [10] Ali, A., Hussain, M.A., Haseeb, M.T., Farid-Ul-Haq, M., Erum, A. and Hussain, M., 2024. Acute toxicity studies of methacrylic acid based composite hydrogel of *Salvia spinosa* seed mucilage: a potential non-toxic candidate for drug delivery. *Cellulose Chemistry and Technology*, 58(1-2), 45-53.
- [11] Ali, A., Hussain, M.A., Haseeb, M.T., Tulain, U.R., Farid-ul-Haq, M., Tabassum, T., Muhammad, G., Hussain, S.Z., Hussain, I. and Erum, A., 2023. Synthesis, characterization, and acute toxicity of pH-responsive *Salvia spinosa* mucilage-co-acrylic acid hydrogel: A smart excipient for drug release applications. *Reactive and Functional Polymers*, 182, 105466.
- [12] Ali, A., Hussain, M.A., Abbas, A., Khan, T.A., Muhammad, G., Haseeb, M.T. and Azhar, I., 2022. Comparative isoconversional thermal analysis and degradation kinetics of *Salvia spinosa* (Kanocha) seed hydrogel and its acetates: a potential matrix for sustained drug release. *Cellulose Chemistry and Technology*, 56(3-4), 239-250.
- [13] Ali, A., Hussain, M.A., Haseeb, M.T., Ashraf, M.U., Farid-ul-Haq, M., Tabassum, T., Muhammad, G. and Abbas, A., 2023. pH-responsive, hemocompatible, and non-toxic polysaccharide-based hydrogel from seeds of *Salvia spinosa* L. for sustained release of febuxostat. *Journal of the Brazilian Chemical Society*, 34, 906-917.
- [14] Rehman, A.U., Maqsood, A., Siddique, A.B., Akhtar, S., Fawy, K.F., Ain, Q.U., Sher, M., Nishan, U., Ahmad, T., Ali, A. and Abbas, A., 2025. From waste to water treatment: Banana peel powder for polystyrene removal with FTIR-based mechanistic understanding. *Journal of Industrial and Engineering Chemistry*. <https://doi.org/10.1016/j.jiec.2025.11.036>.
- [15] Ali, A., Hussain, M.A., Haseeb, M.T., Bukhari, S.N.A., Tabassum, T., Farid-ul-Haq, M. and Sheikh, F.A., 2022. A pH-responsive, biocompatible, and non-toxic citric acid cross-linked polysaccharide-based hydrogel from *Salvia spinosa* L. offering zero-order drug release. *Journal of Drug Delivery Science and Technology*, 69, 103144.
- [16] Amjad, F., Ali, A., Hussain, M.A., Haseeb, M.T., Ajaz, I., Farid-ul-Haq, M., Hussain, S. Z. and Hussain, I., 2025. A superabsorbent and pH-responsive copolymer-hydrogel based on glucomannans from *Ocimum basilicum* (sweet basil): A smart and non-toxic material for intelligent drug delivery. *International Journal of*

- Biological Macromolecules, 315(2), 144452.
- [17] Ali, A., Haseeb, M.T., Hussain, M.A., Muhammad, T., Muhammad, G., Ahmad, N., Alotaibi, N.F., Hussain, S.Z. and Hussain, I., 2022. Extraction optimization of a superporous polysaccharide-based mucilage from *Salvia spinosa* L. Cellulose Chemistry and Technology, 56, 957-969.
- [18] Iqbal, J., Kanwal, M., Siddique, A., Fawy, K.F., Sher, M., Nishan, U., ur Rehman, M.F., Abbas, M.A., Ali, A. and Abbas, A., 2025.  $\beta$ -Cyclodextrin-functionalized silver nanoparticles as a visual probe for selective tetrahydrocannabinol detection via host-guest induced plasmonic shifts. Microchemical Journal, 116177.
- [19] Hussain, M.A., Shahzad, K., Ali, A., Haseeb, M.T. and Hussain, S.Z., 2025. Development of a novel smart biocomposite hydrogel based on dextran, citric acid, and glucoxytan for pH-dependent drug delivery and stimuli-responsive swelling and release. Polymers and Polymer Composites, 33, 09673911251350240.
- [20] Khatoon, M., Ali, A., Hussain, M.A., Haseeb, M.T., Muhammad, G., Sher, M., Hussain, S.Z., Hussain, I. and Iqbal, M., 2025. A chia (*Salvia hispanica* L.) seed mucilage-based glucoxytan-grafted-acrylic acid hydrogel: a smart material for pH-responsive drug delivery systems. Materials Advances, 6(8), 2636-2647.
- [21] Hussain, M.A., Raees, N., Ali, A., Tayyab, M., Muhammd, G., Uroos, M. and Batool, M., 2025. Optimization of rhamnogalacturonan extraction from linseed using RSM and designing a pH-responsive tablet formulation for sustained release of ciprofloxacin. Cellulose Chemistry and Technology, 59, 547-558.
- [22] Hussain, M.A., Taj, T., Ali, A., Haseeb, M.T., Hussain, S.Z., Muhammad, G. and Bukhari, S.N.A., 2025. Cross-linking of hydroxypropylcellulose with flaxseed rhamnogalacturonans Using citric acid produces a hemocompatible biocomposite for pH-responsive rifaximin delivery. Journal of Applied Polymer Science, e57486.
- [23] Hussain, M.A., Abbas, A., Yameen, E., Ali, A., Muhammad, G., Hussain, M. and Shafiq, Z., 2022. Adsorptive removal of  $Pb^{2+}$  and  $Cu^{2+}$  from aqueous solution using an acid modified glucuronoxylan-based adsorbent. Desalination and Water Treatment, 248, 163-175.
- [24] Hussain, M.A., Abbas, A., Habib, M.G., Ali, A., Farid-ul-Haq, M., Hussain, M., Shafiq, Z. and Irfan, M.I., 2021. Adsorptive removal of Ni (II) and Co (II) from aqueous solution using succinate-bonded polysaccharide isolated from *Artemisia vulgaris* seed mucilage. Desalination and Water Treatment, 231, 182-195.
- [25] Ali, A., Hussain, M.A., Abbas, A., Haseeb, M.T., Azhar, I., Muhammad, G., Hussain, S.Z., Hussain, I. and Alotaibi, N.F., 2023. Succinylated *Salvia spinosa* hydrogel: Modification, characterization, cadmium-uptake from spiked high-hardness groundwater and statistical analysis of sorption data. Journal of Molecular Liquids, 376, 121438.
- [26] Zhao, Y., Zheng, Y., Wang, J., Ma, S., Yu, Y., White, W.L., Yang, S., Yang, F. and Lu, J., 2018. Fucoidan extracted from *Undaria pinnatifida*: Source for nutraceuticals/functional foods. Marine Drugs, 16(9), 321.
- [27] Foday Jr, E.H., Bo, B. and Xu, X., 2021. Removal of toxic heavy metals from contaminated aqueous solutions using seaweeds: A review. Sustainability, 13(21), 12311.
- [28] Abbas, A., Hussain, M.A., Amin, M., Tahir, M.N., Jantan, I., Hameed, A. and Bukhari, S.N.A., 2015. Multiple cross-linked hydroxypropylcellulose-succinate-salicylate: prodrug design, characterization, stimuli responsive swelling-deswelling and sustained

- drug release. *RSC Advances*, 5(54), 43440-43448.
- [29] Abbas, A., Siddique, A.B., Batoool, R., Sher, M., Irfan, M.I. and Abbas, M.A., 2023. Isothermal and kinetic modeling for uptake of heavy metal ion from aqueous solution using succinylated polysaccharide. *Starch-Stärke*, 75(5-6), 2200191.
- [30] Wang, T., Liu, W., Xiong, L., Xu, N. and Ni, J., 2013. Influence of pH, ionic strength and humic acid on competitive adsorption of Pb (II), Cd (II) and Cr (III) onto titanate nanotubes. *Chemical Engineering Journal*, 215, 366-374.
- [31] Liu, G., Wang, J., Xue, W., Zhao, J., Wang, J. and Liu, X., 2017. Effect of the size of variable charge soil particles on cadmium accumulation and adsorption. *Journal of Soils and Sediments*, 17(12), 2810-2821.
- [32] Sullivan, D.E., 1979. Van der Waals model of adsorption. *Physical review B*, 20(10), p.3991.
- [33] Kong, W., Yue, Q., Li, Q. and Gao, B., 2019. Adsorption of Cd<sup>2+</sup> on GO/PAA hydrogel and preliminary recycle to GO/PAA-CdS as efficient photocatalyst. *Science of the Total Environment*, 668, 1165-1174.
- [34] Sprynskyy, M., Buszewski, B., Terzyk, A.P. and Namieśnik, J., 2006. Study of the selection mechanism of heavy metal (Pb<sup>2+</sup>, Cu<sup>2+</sup>, Ni<sup>2+</sup>, and Cd<sup>2+</sup>) adsorption on clinoptilolite. *Journal of colloid and interface science*, 304(1), 21-28.
- [35] Travin, S.O., Gromov, O.B., Utrobin, D.V. and Roshchin, A.V., 2019. Kinetic simulation of adsorption isotherms. *Russian Journal of Physical Chemistry B*, 13(6), 975-985.
- [36] Khan, F., Siddique, A.B., Irfan, M.I., Hassan, M.N.U., Sher, M., Alhazmi, H.A., Qramish, A.N., Amin, H.M., Qadir, R. and Abbas, A., 2024. Maleated hydroxyethyl cellulose for the efficient removal of Cd (II) ions from an aqueous solution: isothermal, kinetic and regeneration studies. *Water, Air, & Soil Pollution*, 235(8), 536.
- [37] Moamen, O.A., Murad, G.A. and Hassan, H.S., 2023. Adsorption mechanism and mass transfer modeling of cesium and europium ions adsorption onto hematite-loaded polyacrylamide-gel composite: Pore Volume and Surface Diffusion Model Approach. *Microporous and Mesoporous Materials*, 356, 112564.
- [38] Wang, L., Yu, G., Li, J., Feng, Y., Peng, Y., Zhao, X., Tang, Y. and Zhang, Q., 2019. Stretchable hydrophobic modified alginate double-network nanocomposite hydrogels for sustained release of water-insoluble pesticides. *Journal of Cleaner Production*, 226, 122-132.
- [39] Dursun, A.Y., 2006. A comparative study on determination of the equilibrium, kinetic and thermodynamic parameters of biosorption of copper (II) and lead (II) ions onto pretreated *Aspergillus niger*. *Biochemical Engineering Journal*, 28(2), 187-195.
- [40] Dudev, T. and Lim, C., 2014. Competition among metal ions for protein binding sites: determinants of metal ion selectivity in proteins. *Chemical Reviews*, 114(1), 538-556.
- [41] Tordi, P., Ridi, F., Samorì, P. and Bonini, M., 2025. Cation-alginate complexes and their hydrogels: A powerful toolkit for the development of next-generation sustainable functional materials. *Advanced Functional Materials*, 35(9), 2416390.